



Quantifying and correcting the effect of vertical penetration assumptions on droplet concentration retrievals from passive satellite instruments

Daniel P. Grosvenor¹, Odran Sourdeval², and Robert Wood³

¹School of Earth and Environment, University of Leeds, Leeds, LS2 9JT, UK

²Leipzig Institute for Meteorology, Universität Leipzig, Germany

³Department of Atmospheric Sciences, University of Washington, Seattle, USA

Correspondence to: D. P. Grosvenor

(daniel.p.grosvenor@gmail.com)

Abstract. Droplet concentration (N_d) retrievals from passive satellite retrievals of cloud optical depth (τ) and effective radius (r_e) usually assume the model of an idealised cloud in which the liquid water content (LWC) increases linearly between cloud base and cloud top (i.e., at a fixed fraction of the adiabatic LWC) with a constant N_d profile. Generally it is assumed that the retrieved r_e value is that at the top of the cloud. In reality, barring r_e retrieval biases due to cloud heterogeneity, etc., the 5 retrieved r_e is representative of that lower down in the cloud due to the vertical penetration of photons at the shortwave infra-red wavelengths used to retrieve r_e . This inconsistency will cause an overestimate of N_d (referred to here as the “penetration depth bias”), which this paper quantifies. Here we estimate penetration depths in terms of optical depth below cloud top ($d\tau$) for a range of idealised modelled adiabatic clouds using bispectral retrievals and plane-parallel radiative transfer. We find a tight 10 relationship between $d\tau$ and τ and that a 1-D relationship approximates the modelled data well. Using this relationship we find that $d\tau$ values and hence N_d biases are higher for the 2.1 μm channel r_e retrieval ($r_{e2.1}$) compared to the 3.7 μm one ($r_{e3.7}$). The theoretical bias in the retrieved N_d is likely to be very large for optically thin clouds, nominally approaching infinity for clouds whose τ is close to the penetration depth. The relative N_d bias rapidly reduces as cloud thickness increases, although still remains above 20 % for $\tau < 19.8$ and $\tau < 7.7$ for $r_{e2.1}$ and $r_{e3.7}$, respectively.

The magnitude of the N_d bias upon climatological N_d data sets is estimated globally using one year of daily MODIS (MODerate Imaging Spectroradiometer) data. Screening criteria are applied that are consistent with those required to help ensure accurate N_d retrievals. The results show that the SE Atlantic, SE Pacific (where the VOCALS field campaign took place) and Californian stratocumulus regions produce fairly large overestimates due to the penetration depth bias with mean biases of 35–38 % for $r_{e2.1}$ and 17–20 % for $r_{e3.7}$. For the other stratocumulus regions examined the errors are smaller (25–30 % for $r_{e2.1}$ and 11–14 % for $r_{e3.7}$). Significant time variability in the percentage errors is also found with regional mean standard 20 deviations of 20–40 % of the regional mean percentage error for $r_{e2.1}$ and 40–60 % for $r_{e3.7}$. This shows that it is important to apply a daily correction to N_d for the penetration depth error rather than a time-mean correction when examining daily data. We also examine the seasonal variation of the bias and find that the biases in the SE Atlantic, SE Pacific and Californian



stratocumulus regions exhibit the most seasonality with the largest errors occurring in the December, January, February (DJF) season.

We show that this effect can be corrected for by simply removing $d\tau$ from the observed τ and provide a function to allow the calculation of $d\tau$ from τ . However, in reality this error will be combined with a number of other errors that affect both the 5 r_e and τ , which are potentially larger and may compensate or enhance the bias due to vertical penetration depth.

1 Introduction

Clouds have a major impact on Earth's radiative balance (Hartmann et al., 1992) and small changes in their properties are predicted to have large radiative impacts (e.g., Latham et al., 2008). The amount of shortwave (SW) flux reflected by fully overcast warm (liquid water) clouds for a given sun and scattering angle, or the reflectance of a cloud, is primarily determined 10 by the cloud optical depth (τ), which in turn can often be characterized by the liquid water path (LWP, the vertical integral of liquid water content) and the cloud droplet number concentration (N_d). For a given cloud updraft, N_d is determined by the number concentration and physico-chemical properties of aerosols. Thus, couching cloud reflectance in terms of N_d links the cloud albedo to aerosol and microphysical effects via the Twomey (1974) effect making N_d a very useful quantity to determine observationally. N_d can also influence cloud macrophysical feedbacks via its control on rain formation (Albrecht, 15 Stevens et al., 1998; Ackerman et al., 2004; Berner et al., 2013; Feingold et al., 2015) and stratocumulus cloud top entrainment (Ackerman et al., 2004; Bretherton et al., 2007; Hill et al., 2009).

Satellite observations of clouds and N_d are immensely useful for studying clouds, cloud–aerosol interactions and for model evaluation since they afford large spatial-temporal coverage. A method to obtain N_d from passive satellite observations (e.g., from MODIS (MODerate Imaging Spectroradiometer); Salomonson et al. (1998)) of τ and the cloud droplet effective radius 20 (r_e) for stratiform liquid clouds has been previously demonstrated (Han et al., 1998; Brenguier et al., 2000; Nakajima et al., 2001; Szczodrak et al., 2001; Boers et al., 2006; Quaas et al., 2006; Bennartz, 2007; Grosvenor and Wood, 2014; Bennartz and Rausch, 2017) and is described further below. In cloudy environments, aerosol optical depths cannot be retrieved from satellite making cloud property observations such as N_d and the cloud droplet effective radius (r_e) the only useful indicator of the influence of aerosol on clouds. An advantage to using N_d rather than r_e to study cloud–aerosol interactions is that r_e is also 25 determined by the cloud water content and thus is a function of cloud macrophysical properties. N_d on the other hand is only weakly controlled by cloud macrophysics allowing some separation of microphysical and macrophysical effects.

However, retrievals of N_d from space are still somewhat experimental and there is a lack of comprehensive validation of the retrievals and the assumptions required. There is a need to characterize and quantify the associated errors; in this paper we focus on doing this for one source of N_d error using a one–year N_d data set for stratocumulus clouds from MODIS.



30 **2 The vertical penetration depth N_d bias and the adiabatic N_d retrieval model**

N_d is retrieved from passive satellite retrievals of r_e and τ using an adiabatic cloud model that is described below. However, as shown in Platnick (2000); Bennartz and Rausch (2017), for a retrieval free from other error sources (e.g. those due to cloud heterogeneity), the retrieved r_e is representative of the r_e value lower down in the cloud due to the vertical penetration of photons at the shortwave infra-red wavelengths used to retrieve r_e . In contrast, the retrieved τ is comprised of contributions 5 from the extinction coefficient $\beta_{ext}(h)$, where h represents height from cloud base, throughout the whole cloud profile :-

$$\tau = \int_0^H \beta_{ext}(h) dh. \quad (1)$$

Here $h=0$ represents cloud base and $h=H$ is cloud top.

$\beta_{ext}(h)$ is defined as :-

$$\beta_{ext}(h) = \pi \int_0^\infty Q_{ext}(r) r^2 n(r) dr, \quad (2)$$

10 where r is the droplet radius and $n(r)$ is the droplet size number distribution within a cloud unit volume such that $N_d = \int_0^\infty n(r) dr$. $Q_{ext}(r)$ represents the ratio between the extinction and the geometric cross sections of a given droplet and can be approximated by its asymptotic value of 2 (van de Hulst, 1957) since droplet radii are generally much larger than the wavelength of light concerned (typically 0.6 to 0.85 μm) such that the geometric optics limit is almost reached.

r_e and liquid water content LWC at a given height are respectively defined as:

$$15 \quad r_e(h) = \frac{\int_0^\infty r^3 n(r) dr}{\int_0^\infty r^2 n(r) dr} \quad (3)$$

and

$$LWC(h) = \frac{4\pi\rho_w}{3} \int_0^\infty r^3 n(r) dr, \quad (4)$$

where ρ_w is the density of liquid water. Combining Eqns. 3 and 4 and inserting into Eqn. 2 gives :-

$$\beta_{ext}(h) = \frac{3Q_{ext}}{4\rho_w} \frac{LWC(h)}{r_e(h)} \quad (5)$$

20 To determine the form of $r_e(h)$ in the above equation in terms of $L(h)$ and $N_d(h)$ we can utilize the fact that the “ k ” value,

$$k = \left(\frac{r_v}{r_e} \right)^3, \quad (6)$$



which is a measure of the width of the droplet size distribution, has been shown to be approximately constant in stratocumulus clouds (Martin et al., 1994; Pawlowska et al., 2006; Painemal and Zuidema, 2011). In this study we adopt a value of $k = 0.8$, which is the most commonly used value in previous studies that perform N_d retrievals (e.g., Bennartz, 2007; Painemal and Zuidema, 2011) in stratocumulus. r_v is the volume radius, defined as :-

$$r_v(h)^3 = \frac{1}{N_d(h)} \int_0^\infty r^3 n(r) dr = \frac{3LWC(h)}{4\pi\rho_w N_d(h)} = kr_e(h)^3, \quad (7)$$

5 where we have used Eqn. 4 to insert LWC and Eqn. 6 to write r_v as a function of k and r_e . Now we utilize the assumptions that $N_d(h)$ is constant with height and that LWC(h) is a constant fraction, f_{ad} , of adiabatic. The latter equates to :-

$$LWC(h) = f_{ad}c_w h, \quad (8)$$

where c_w is the rate of increase of LWC with height ($dLWC/dz$, with units kgm^{-4}) for a moist adiabatic ascent and is referred to as the “condensation rate” in Brenguier et al. (2000), or the “water content lapse rate” in Painemal and Zuidema (2011). See
 10 Ahmad et al. (2013) for a derivation. c_w is a constant for a given temperature and pressure. Allowing these assumptions, using Eqn. 7 to substitute for r_e in Eqn. 5 and combining with Eqns. 1 and 8 we can write :-

$$\begin{aligned} \tau^* &= \int_0^{H^*} Q_{\text{ext}} \left(\frac{3f_{ad}c_w}{4\rho_w} \right)^{2/3} (N_d\pi k)^{1/3} h^{2/3} dh \\ &= \frac{3Q_{\text{ext}}}{5} \left(\frac{3f_{ad}c_w}{4\rho_w} \right)^{2/3} (N_d\pi k)^{1/3} H^{*5/3} \end{aligned} \quad (9)$$

At this stage, H^* is any arbitrary height above cloud base and τ^* is thus the optical depth between the cloud base and that height. H^* can be expressed as a function of $r_e(H^*)$, k , N_d and some constants by using Eqns. 7 and 8. Then, given $r_e(H^*)$ and τ^* , N_d can be calculated as follows :-

$$N_d = \frac{\sqrt{5}}{2\pi k} \left(\frac{f_{ad}c_w \tau^*}{Q_{\text{ext}}\rho_w r_e(H^*)^5} \right)^{1/2} \quad (10)$$

Generally, when retrieving N_d it is assumed that the r_e obtained from satellite is representative of that from cloud top, i.e., $r_e(H^*)=r_e(H)$ (e.g. Bennartz, 2007; Painemal and Zuidema, 2011). This would then mean that τ^* is the full cloud optical depth (τ) as retrieved by the satellite and thus could be used in Eqn. 10 above to obtain N_d . However, since the r_e obtained by satellite
 20 is actually equal to $r_e(H^*)$ then $\tau^* < \tau$ and thus τ^* should be used in Eqn. 10 instead of the retrieved τ ; the problem lies in the fact that τ^* is unknown. However, in this paper we fit a simple function for τ^* as a function of τ based on radiative transfer modelling of a variety of idealised clouds. Then we estimate the error introduced in N_d retrievals for one year of MODIS data due to the assumptions of $r_e(H^*)=r_e(H)$ and $\tau^*=\tau$, on the assumption that there are no other biases affecting the r_e retrieval. We label this bias the “vertical penetration bias”.



3 Data and Methods

3.1 Calculation of $d\tau$

In order to calculate

$$d\tau = \tau - \tau^* \quad (11)$$

5 we have performed r_e retrievals on idealised clouds using a similar algorithm to that used for MODIS retrievals. We produced idealised clouds that span a large range of stratocumulus-like clouds as represented by combinations of N_d and LWP. We chose 41 values between $N_d=10$ and 1000 cm^{-3} that were equally spaced in log space and 91 values between $\text{LWP}=20$ and 200 gm^{-2} spaced equally in linear space. All of the possible combinations from this sampling were used to sample the 2-D (N_d , LWP) phase space. For each combination, discretized adiabatic model profiles following the form of those described in Section 1
10 (i.e., with a vertically constant N_d and LWC that increases linearly with height) were generated using $c_w=1.81 \times 10^{-6} \text{ kg m}^{-4}$, $f_{ad}=0.8$ and using a vertical spacing of 1 m. The droplet size distributions at each height were represented by a modified gamma distribution with a k value of 0.72, i.e. representative of an effective variance of 0.1. 1-D radiative transfer (RT) calculations, assuming plane-parallel clouds, were performed on these profiles using the DISORT (Discrete Ordinates Radiative Transfer Program; Stamnes et al., 1988) radiation code in order to simulate reflectances at wavelengths of 0.86, 2.1 and $3.7 \mu\text{m}$,
15 matching those measured by MODIS to retrieve τ and r_e . The RT calculations were performed assuming a black surface, a clear atmosphere (i.e. gaseous absorption is neglected), using a solar zenith angle of 20° and a nadir viewing angle. These reflectances were then used to retrieve τ and r_e values using the Nakajima and King (1990) bi-spectral method, as operationally used by MODIS. To do so, a lookup table was built from reflectances similarly calculated for a range of clouds that were assumed to be plane-parallel in nature, as assumed for the operational MODIS retrievals; i.e. these clouds were uniform in the vertical
20 and horizontal with infinite horizontal extent. Again, a black surface and a k value of 0.72 were assumed along with the same viewing geometry as for the RT calculations on the adiabatic clouds. A fixed depth of 1 km was assumed with cloud base at an altitude of 1 km and cloud top at 2 km, although the cloud depth has no major effect on the reflectances generated. $d\tau$ was then calculated by choosing the value of the model profile of τ , as measured from cloud top downwards, that corresponded to the value of the model profile of r_e that matched the retrieved r_e .
25 Figure 1a shows a 2-D histogram of $d\tau$ values as a function of τ for the $2.1 \mu\text{m}$ retrieval. It shows that when plotted in this way $d\tau$ forms a fairly tight relationship with τ so that for a given τ only a small range of $d\tau$ values are possible. This suggests that the relationship can be parameterized based upon a 1-D relationship fitted to this data with little loss of accuracy. The mean value of each τ bin is also plotted (after smoothing over τ windows of 0.2) and this is the relationship used in this paper. $d\tau$ is seen to increase with τ with a gradient that decreases with τ . A 4th order polynomial curve can be fitted (using the least
30 squares method) to this mean value relationship that takes the form:-

$$d\tau = a_4\tau^4 + a_3\tau^3 + a_2\tau^2 + a_1\tau + a_0 \quad (12)$$



The coefficients of this fit and for the 3.7 μm retrieval are given in Table 1 along with the maximum absolute τ error for the fit for the range shown. The curve (white line in Fig. 1a) fits the mean data well with a maximum absolute difference of 0.09, although there will be some error when using this relationship (or the mean value relationship) due to the spread in the $d\tau$ values seen in the underlying histogram.

Table 1. Coefficients for the fitting curve (Eqn. 12) to estimate the mean $d\tau$ value as a function of τ . The maximum absolute error from the fit is also shown.

Retrieval wavelength	a_4	a_3	a_2	a_1	a_0	Max abs τ error
2.1 μm	-3.174e-06	3.931e-04	-0.021	0.5754	0.3216	0.09
3.7 μm	-1.281e-05	1.099e-03	-0.03304	0.4168	0.6005	0.14

Figure 1b shows the same results for the 3.7 μm retrieval. Again a tight 1-D relationship is suggested with a $d\tau$ value that increases with τ . Here, though, the curve flattens off much more rapidly, so that by $\tau=7.5$ there is little dependence of $d\tau$ on τ and $d\tau$ saturates at a mean value of ~ 2.6 . The fit estimate for the mean curve (Eqn. 12 and Table 1) again matches the actual curve closely with a maximum absolute error in $d\tau$ of 0.14.

3.2 MODIS data

For the MODIS data we use one year (2008) of MODIS Aqua data and follow a similar methodology to that used in Grosvenor and Wood (2014) in order to create a data set akin to the MODIS L3 product (King et al., 1997; Oreopoulos, 2005). We processed MODIS collection 5.1 joint-L2 swaths into $1^\circ \times 1^\circ$ grid boxes. Joint-L2 swaths are sub-sampled versions of the full L2 swaths (sampling every 5th 1 km pixel) that also contains fewer parameters. We process the data from L2 to L3 in order to allow the filtering out of data at high solar zenith angles and to provide r_e retrievals from both the 2.1 μm and 3.7 μm MODIS channels, hereafter referred to as $r_{e2.1}$ and $r_{e3.7}$, respectively.

For this work we relax the screening methodology slightly from that used in Grosvenor and Wood (2014) since here we are interested in the effects of the vertical penetration N_d bias upon a more general global data set. We applied the following restrictions to each $1^\circ \times 1^\circ$ sample that goes into the daily average (since multiple overpasses per day are possible) in order to attempt to remove some artifacts that may cause biases:

1. At least 50 joint-L2 1 km resolution pixels from the MODIS swath that did not suffer from sunglint were required to have been sampled within each gridbox.
2. At least 80 % of the available (non-sunglint) pixels were required to be of liquid phase based upon the “primary cloud retrieval phase flag”. Analysis was only performed on these pixels. A high cloud fraction helps to ensure that the clouds are not broken, since broken clouds are known to cause biases in retrieved optical properties due to photon scattering

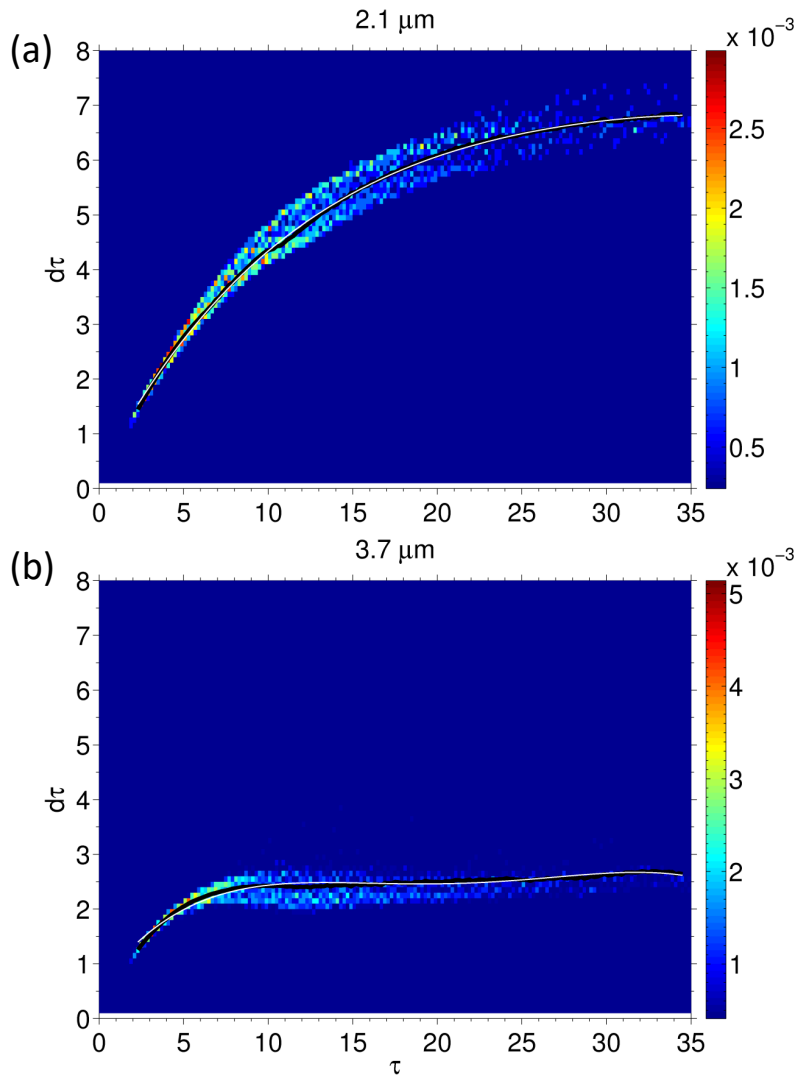


Figure 1. 2D histogram of $d\tau$ as a function of τ for a range of clouds (see text) for the $2.1 \mu\text{m}$ r_e retrieval (a) and the $3.7 \mu\text{m}$ retrieval (b). The black line is the mean $d\tau$ in each τ bin after smoothing over τ interval windows of 0.2. The white line is the fit to the mean curve using Eqn. 12.

through the sides of clouds. Often retrievals of N_d are restricted to high cloud fraction fields for this reason (B07; PZ11) and so we focus on such datapoints here.

3. Only the pixels remaining after (2) for which the “cloud mask status” indicated that the cloud mask could be determined, the “cloud mask cloudiness flag” was set to “confident cloudy”, successful simultaneous retrievals of both τ and r_e



for the $2.1\mu\text{m}$ channel were performed and the cloud water path confidence from the MODIS L2 quality flags was designated as “very good confidence” (the highest level possible) were used. This is a little different from the official MODIS L3 product where a set of cloud products are provided that are weighted using the quality assurance flags. Rather than weighting our L3-like product with the QA flags we have simply restricted our analysis to pixels with the highest confidence for water path.

4. The mean $1^\circ \times 1^\circ$ cloud top height (CTH) is restricted to values lower than 3.2 km. This is done both to avoid deeper
5 clouds for which N_d retrievals are likely to be problematic due to the increased likelihood of a breakdown of the as-
sumptions required to estimate N_d , such as a constant fraction of the adiabatic value for LWC and vertically constant N_d ,
10 as well increased retrieval issues due to cloud heterogeneity. CTH is calculated from the MODIS $1^\circ \times 1^\circ$ mean cloud
top temperature (CTT) and the sea surface temperature (SST) using the method of Zuidema et al. (2009). SST data was
obtained from the v2 of the NOAA Optimum Interpolation (OI) Sea Surface Temperature data set (NOAA_OI_SST_V2)
that provides weekly SST data at $1^\circ \times 1^\circ$ resolution. This was interpolated to daily data on the assumption that SST does
not vary significantly over sub-weekly timescales.
5. The mean $1^\circ \times 1^\circ$ solar zenith angle (SZA) was restricted to $\leq 65^\circ$ following the identification of biases in the retrieved
 τ , r_e and N_d at high SZAs (Grosvenor and Wood, 2014).
6. $1^\circ \times 1^\circ$ grid-boxes were rejected if the maximum sea-ice areal coverage over a moving two week window exceeded
15 0.001 %. The sea-ice data used was the daily $1^\circ \times 1^\circ$ version of the “Sea Ice Concentrations from Nimbus-7 SMMR and
DMSP SSM/I-SSMIS Passive Microwave Data, Version 1” data set (Cavalieri et al., 1996).
7. Only pixels with $\tau > 5$ were considered for the N_d data set due to larger uncertainties from instrument error and other
sources of reflectance error for τ and r_e retrievals at low τ (Zhang and Plantnick, 2011; Sourdeval et al., 2016).

Figure 2a shows the number of days from the year of data examined in this study (year 2008) that fulfilled the above criteria
20 and thus are likely to produce a good N_d retrieval. Regions with high numbers of days where useful N_d retrievals can be
made have been selected for closer examination in this study; they are listed in Table 2 along with information on the mean and
maximum numbers of days of good data and some statistics on the N_d biases that will be described later. The permanent marine
stratocumulus decks are among those selected, namely those: in the SE Pacific off the western coast of S. America (Region
#1); in the SE Atlantic off the western coast of southern Africa (Region #2); off the coast of California and the Baja Peninsula
25 (Region #3); in the Bering Sea off the SW coast of Alaska (Region #6); and in the Barents Sea to the north of Scandinavia
(Region #8). These regions are where the highest numbers of selected days occur with values ranging up to a maximum of 141
days (for the Bering Sea region). The Barents Sea region has the lowest maximum number of days out of this group, reflecting
the fact that N_d retrievals cannot be made during a lot of the winter season in this region due to a lack of sunlight. The Southern
30 Ocean (Region #5) and the NW Atlantic (Region #7) regions frequently produce stratocumulus, although it is often associated
with the cold sectors of cyclones and so its location from day to day is more transient. These regions are also affected by high
solar zenith angles in the winter seasons, which also restricts the number of retrievals possible there. The East China Sea region



(Region #4) produces the lowest mean and maximum numbers of days since the stratocumulus areas are mostly restricted to near the coast and occur mostly in the winter season.

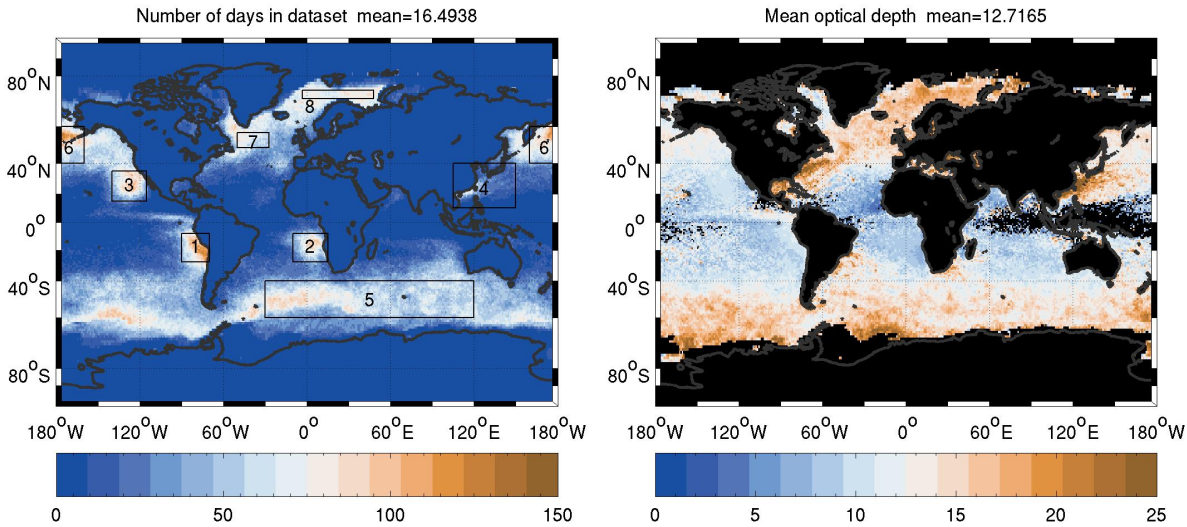


Figure 2. Left: Number of days in 2008 that fulfilled the criteria required to be counted as a valid N_d retrieval. See the text for details on the criteria. Various regions of interest are also denoted by the boxes and numbers. Right: Mean optical depth for data set with only filtering criteria 1-6 applied (see text); i.e., the $\tau > 5$ restriction was not applied.

Following this screening, the $1^\circ \times 1^\circ$ gridboxes associated with each MODIS Aqua overpass were averaged into daily mean values. N_d was then calculated using Eqn. 10 from the $1^\circ \times 1^\circ$ daily mean τ , r_e and CTT. N_d was calculated for both $r_{e2.1}$ and $r_{e3.7}$. This was done both by using the retrieved τ value instead of τ^* in Eqn. 10 (i.e., assuming that $r_e(H^*)=r_e(H)$ as is often assumed for N_d retrievals) and by estimating τ^* using the retrieved τ along with the $d\tau$ values that were calculated as described above. This therefore gives N_d data sets for the “standard” method and a corrected method, allowing the differences 5 between the two to be examined.

4 Results

Following Eqn 10, the ratio between the uncorrected and corrected N_d values can be shown to be :-

$$\frac{N_{d(uncorrected)}}{N_{d(corrected)}} = \left(\frac{\tau}{\tau^*} \right)^{1/2} = \left(\frac{\tau}{\tau - d\tau} \right)^{1/2} \quad (13)$$

The equation shows that, for a constant $d\tau$, the relative N_d bias due to an uncorrected τ value would increase with decreasing 10 τ as $\tau - d\tau$ approaches zero. Figure 3 shows how the relative bias varies as a function of retrieved τ when using the $d\tau$ values based on those from Fig. 1 (mean curve, black line).



At $\tau=5$ the relative error is 50% for the $r_{e2.1}$ retrieval and 30% for the $r_{e3.7}$ retrieval. At higher τ the errors reduce rapidly, but remain above 10% for the $r_{e2.1}$ retrieval over the τ range shown. For the $r_{e3.7}$ retrieval the relative error drops below 10% for $\tau > \sim 15$. Thus, the overall degree of error due to this effect will be determined by the distribution of τ for the regions of
 15 interest, which we take into consideration here using MODIS data for a representative N_d data set.

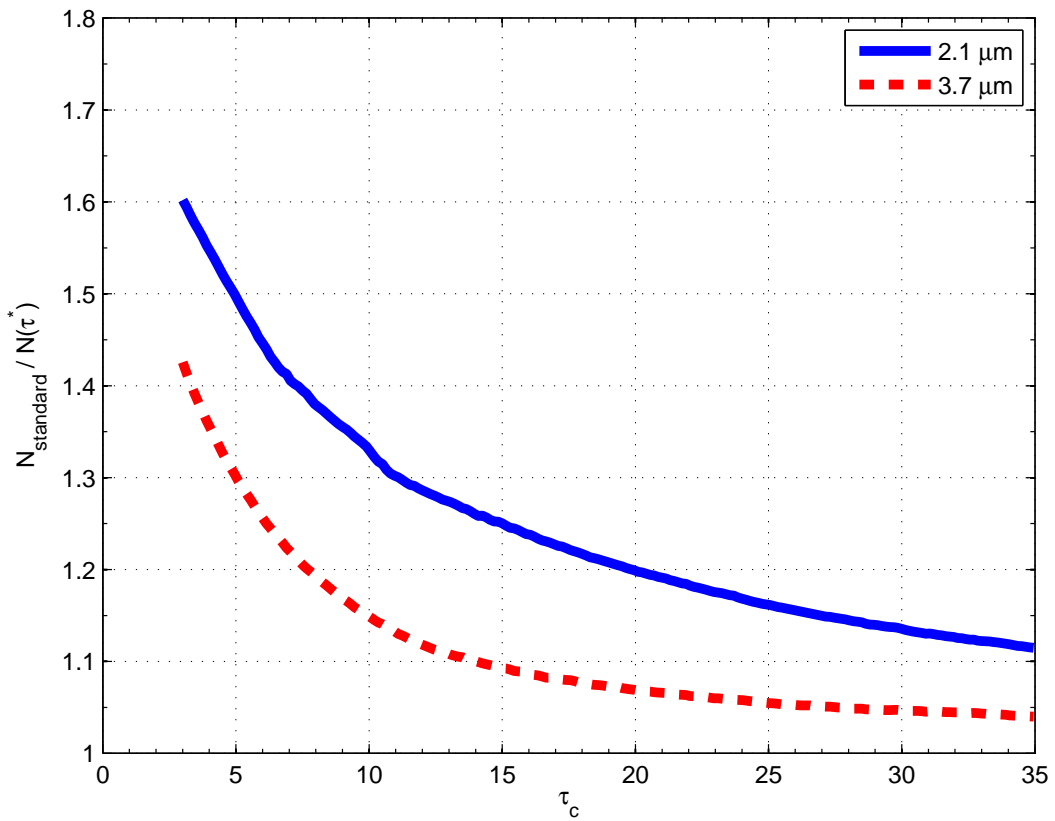


Figure 3. The ratios of N_d values from the standard MODIS calculation (using $\tau^*=\tau$, see Eqn. 10) to those from the corrected calculation (using $\tau^*=\tau-d\tau$; the $d\tau$ values used are those shown by the black line in Fig. 1) vs retrieved τ .

Figure 2b shows the time-mean τ for the data set as filtered by criteria 1-6 above; i.e. without the $\tau > 5$ restriction. Table 2 lists the regional means of these time-mean values along with the regional means of the standard deviations of τ over time. It shows that the mean τ values of the tropical and sub-tropical regions are generally lower than those at higher latitudes. The East China Sea, Barents Sea, NW Atlantic and Southern Ocean regions exhibit the highest mean τ values out of those examined
 5 and so should be expected to show the lowest N_d biases due to the vertical penetration effect. The SE Atlantic region (and the region to the west of Africa in general) show low τ and can be expected to give high N_d biases. Table 2 also lists the fraction of days for which $\tau \leq 10$ ($f_{\tau \leq 10}$). $\tau=10$ is the value above which N_d biases drop below 33% for the 2.1 μm retrieval and below



15 % for $r_{e3.7}$ according to Fig. 3. Thus $f_{\tau \leq 10}$ indicates the fraction of days for which daily N_d biases will be greater than 33% for that channel. The values in the table indicate that even in the least affected region (Barents Sea) this will occur for 23% of
 10 the days. For the SE Atlantic and SE Pacific region the percentages rise to 72% and 55% of the days, respectively. Thus, the vertical penetration depth N_d bias is prevalent in all regions for which N_d data sets are likely to be used, and particularly so in the sub-tropical stratocumulus regions where N_d retrievals have been widely used and studied.

The overall bias is now estimated using one year of actual MODIS data in order to obtain a realistic distribution of τ values. However, it should be noted that the data set used is deliberately filtered in order to only retain datapoints that are likely to give useful N_d data, namely low liquid clouds with extensive $1 \times 1^\circ$ cloud fractions; i.e., predominately stratocumulus. This is done
 5 in order to assess biases for the types of clouds that N_d data sets will typically be used to study.

Table 2. Regional statistics for the various marine stratocumulus regions shown in Fig. 2. Shown are the mean and maximum number of days that fulfill the screening criteria in order to be considered as useful N_d retrievals; the regional means and standard deviations (σ) of the time-averaged optical depths (τ) for the screened data set; the regional mean of the fraction of days for which $\tau \leq 10$ ($f_{\tau \leq 10}$), which is calculated using only data from gridpoints for which the number of days with N_d data was ≥ 15 ; regional means of the predicted time-mean percentage biases in N_d due to the vertical penetration depth error; and regional means of the relative (percentage) standard deviations (over time) of the percentage N_d biases (i.e., regional means of the values in Fig. 5). Bias results are shown for both the $2.1 \mu\text{m}$ and the $3.7 \mu\text{m}$ r_e retrievals.

#	Region name	Mean no. days	Max no. days	2.1 μm % biases			3.7 μm % biases			
				Mean τ	σ_{τ}	$f_{\tau \leq 10}$	Mean bias (%)	σ (%)	Mean bias (%)	
1	SE Pacific	72.1	138	10.2	3.95	0.55	34.6	24.0	17.0	40.5
2	SE Atlantic	59.7	119	8.5	3.34	0.72	38.4	22.3	20.2	37.7
3	California	68.0	120	10.0	4.27	0.58	35.4	25.9	17.8	43.9
4	East China Sea	13.6	86	17.5	10.25	0.28	27.4	40.5	12.7	60.3
5	Southern Ocean	60.6	103	13.8	7.68	0.37	29.9	34.0	13.9	53.7
6	Bering Sea	76.0	146	13.3	6.94	0.38	30.4	31.7	14.1	50.8
7	NW Atlantic	66.0	91	15.6	9.29	0.31	27.9	36.5	12.6	56.3
8	Barents Sea	76.2	89	17.8	9.94	0.23	25.4	39.6	11.0	60.1

Fig. 4 shows a map of the mean percentage biases and Table 2 gives the regional means of the values in the map. Considering firstly the biases for the $r_{e2.1}$ retrieval, the biases are highest in the tropics and sub-tropics. The regional mean bias is 38% for the SE Atlantic region (Region #2), which is the stratocumulus region that seems to suffer the most. The biases are a little lower for the other major stratocumulus regions; e.g. for the SE Pacific region (Region #1) and the Californian region (Region
 10 #3) the mean biases are 35%, although the biases increase further west where the dominant cloud regime tends to shift towards trade cumulus clouds. The remaining regions all have mean biases of 25–30%. The Barents Sea region (Region #8) has a value



of only 25%, representing the stratocumulus region with lowest mean bias. These results indicate higher τ values for the clouds in the East China Sea, Southern Ocean, Bering Sea, NW Atlantic and Barents Sea regions relative to the Californian and S.E. Pacific stratocumulus regions, with the SE Atlantic region exhibiting the lowest τ values. This is confirmed by the mean τ values shown in Table 2. The biases for the $r_{e3.7}$ retrieval display the same spatial patterns as for $r_{e2.1}$, but are significantly lower; the mean value in the region with the maximum bias (SE Atlantic, Region #2) is 20% and that in the region with the lowest bias (Barents Sea, Region #8) is 11%.

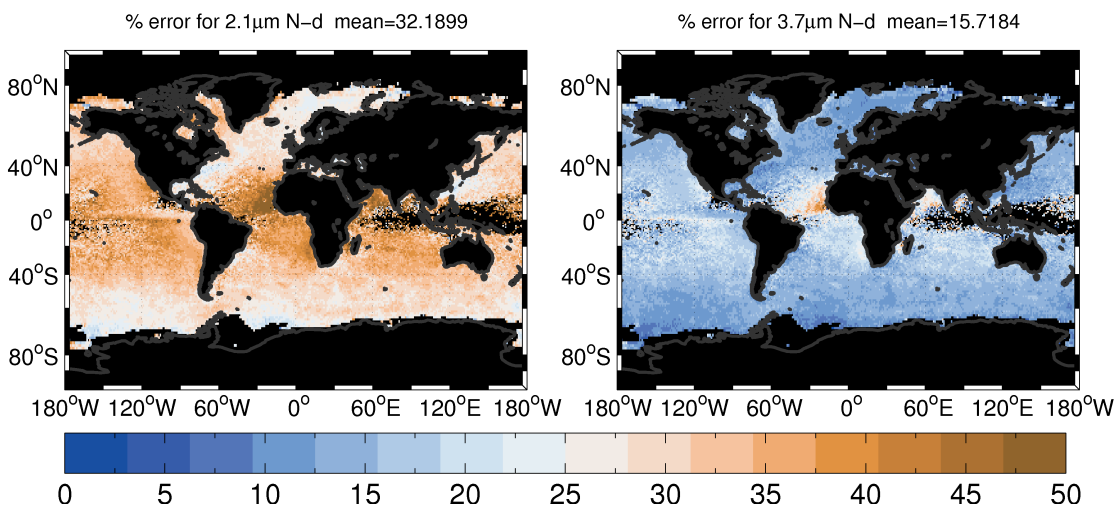


Figure 4. Maps of the annual mean percentage error for uncorrected N_d retrievals using a year (2008) of daily MODIS data that has been filtered to select data points in which N_d retrievals are favourable and therefore most likely to be used for N_d data sets (see text for details). The left plot shows the results for the $r_{e2.1}$ retrieval and the right for the $r_{e3.7}$ one.

It is also useful to know how variable the biases are from day to day for a given point in space since this will determine how useful the application of a single offset bias correction might be for correcting N_d biases for daily data. Figure 5 shows the time variability of the bias in the form of the relative standard deviations (over time) of the percentage N_d biases. It reveals that the percentage bias in N_d generally has a larger relative standard deviation at latitudes above around 40° with values typically ranging up to around 30–50% (of the mean percentage N_d bias) for the $2.1 \mu\text{m}$ retrieval. Relative variability is greater for the $3.7 \mu\text{m}$ retrieval, perhaps due to the much lower mean percentage errors. Some of the selected regions show more variability than others, in particular the Barents Sea and East China Sea regions.

Table 2 gives the regional means of the relative standard deviations revealing values that range from approximately 20 to 40% of the mean percentage biases for the $2.1 \mu\text{m}$ retrieval and 40–60% for the $3.7 \mu\text{m}$ one. This shows that the application of a single annual mean offset bias correction is likely to lead to fairly large biases for the N_d estimates for individual days for regions where the mean N_d errors are significant. If daily data is used to determine relationships between cloud properties and



N_d without correcting for the biases examined here then significant variability in N_d might be introduced that may affect those
 15 relationships via non-linear effects.

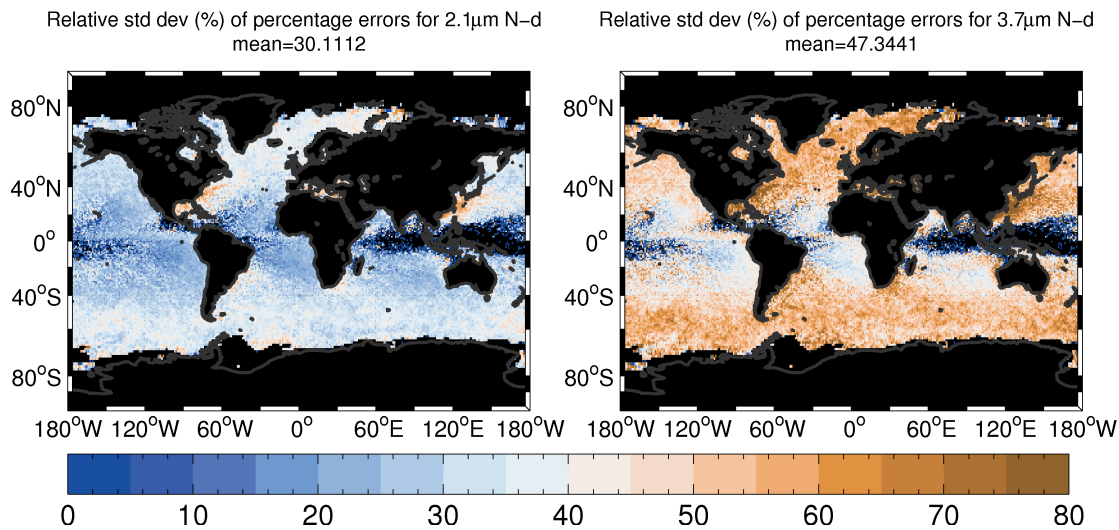


Figure 5. As for Fig. 4 except showing the relative (as a percentage) standard deviation of the percentage N_d bias over time.

Fig. 6 shows how the percentage N_d biases change with season for the $r_{e2.1}$ retrieval only. Interestingly, the highest biases tend to occur in the DJF season for the SE Pacific and SE Atlantic stratocumulus regions, indicating that τ values are lower in DJF for those seasons. The SON season also generally produces higher biases than MAM and JJA for those regions, particularly for SE Pacific. For the East China Sea region the biases are lower in SON and DJF seasons than in the other seasons. We note that there is little data in this region for JJA since there are few low-altitude clouds with large regional liquid cloud fraction there in this season. The other regions either do not show a large amount of seasonal variability, or N_d data is only available for
 5 part of the year due to a lack of sunlight in the winter months.

5 Discussion

There are some caveats to the results that we presented here that we now discuss. We have shown that, theoretically, the effect of retrieving a lower r_e than the cloud top r_e that is assumed in the N_d retrieval can be corrected for by simply removing $d\tau$ from the observed τ . However, this rests upon $d\tau$ having the dependence upon τ shown in Fig. 3 across all of the cloud types
 10 relevant for the N_d data set. This relationship was based on the retrieved r_e for a range of clouds, although only for a nadir viewing angle and a solar zenith angle of 20°. Platnick (2000) showed that $d\tau$ has some dependence on viewing geometry and so the consideration of a wider range of view and solar zenith angles should ideally be made.

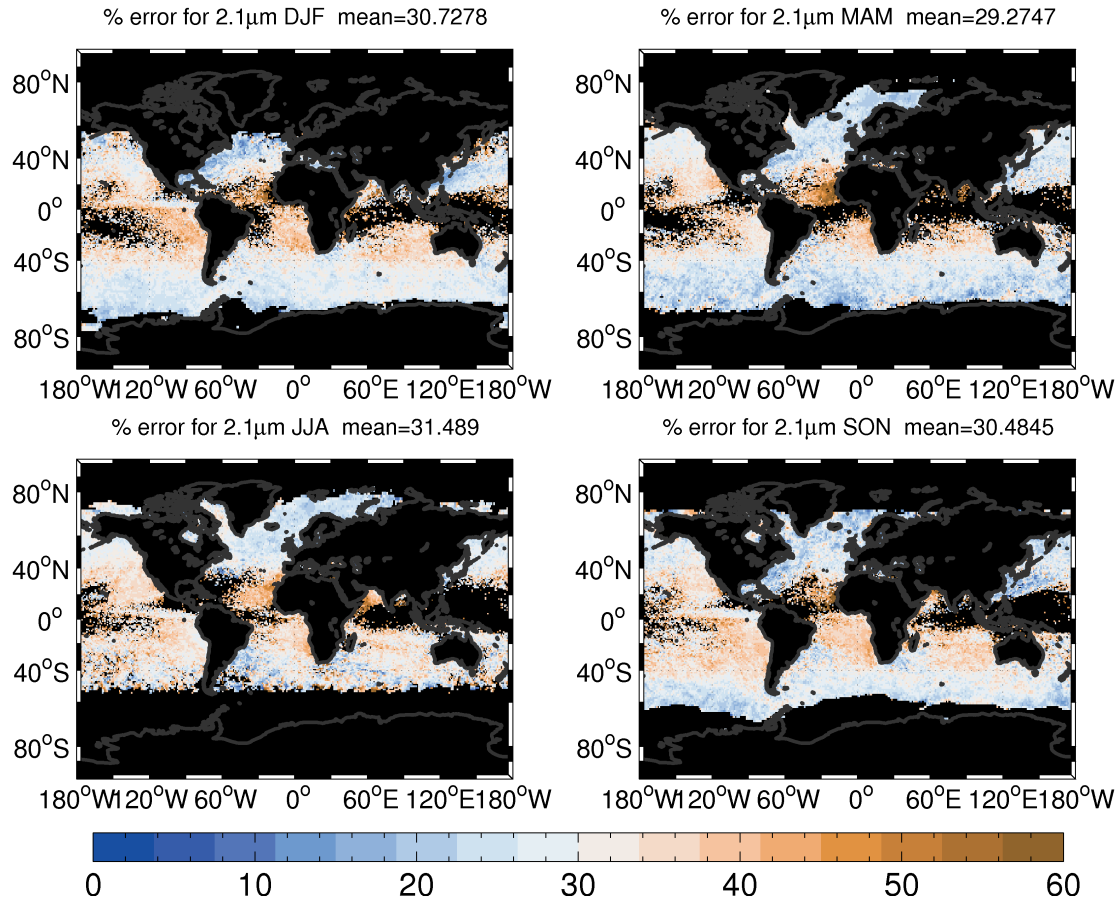


Figure 6. Seasonal mean percentage N_d biases for the $r_{e2.1}$ retrieval only.

The modelling of the idealised clouds and the correction rests on the assumption that r_e increases monotonically with height within the cloud (following the adiabatic assumption), but there is some suggestion that the development of precipitation-sized droplets might lead to larger droplets being preferentially found below cloud top (Chang and Li, 2002; Nakajima et al., 2010a, b; Suzuki et al., 2010). However, Zhang et al. (2012) found that MODIS retrievals of r_e performed on model generated clouds were not significantly affected by the presence of precipitation. Also, during the VOCALS field campaign in the SE Pacific region, aircraft observations showed that r_e generally did increase with height up to cloud top (Painemal and Zuidema, 2011), indicating that this is not a problem at least for the near-coastal clouds tested. Further offshore the likelihood of precipitation increases as clouds become more cumulus-like and so for those clouds the issue may be greater and hence more caution should be exercised when interpreting the results presented here for such regions.

It is also clear that the suggested correction for the vertical penetration effect should only be applied to the retrievals of N_d with consideration of other bias sources. These other potential error sources are numerous and include r_e biases due to



5 sub-pixel heterogeneity (Zhang and Plantnick, 2011; Zhang et al., 2012, 2016); 3D radiative effects (Marshak et al., 2006);
assumptions regarding the degree of cloud adiabaticity (f_{ad} in Eqn. 10; Janssen et al., 2011; Merk et al., 2016); the choice of
 k value (assumed constant; Brenguier et al., 2011; Merk et al., 2016); the assumption of a vertically uniform N_d ; the assumed
droplet size distribution shape and width (Zhang, 2013); viewing geometry effects (Várnai and Davies, 1999; Horváth, 2004;
Várnai and Marshak, 2007; Kato and Marshak, 2009; Liang et al., 2009; Di Girolamo et al., 2010; Maddux et al., 2010; Liang
10 and Girolamo, 2013; Grosvenor and Wood, 2014; Liang et al., 2015; Bennartz and Rausch, 2017); upper level cloud and aerosol
layers (Haywood et al., 2004; Bennartz and Harshvardhan, 2007; Davis et al., 2009; Meyer et al., 2013; Adebiyi et al., 2015;
Sourdeval et al., 2013, 2016), etc. These errors have the potential to bias N_d in a way that opposes the positive bias expected
5 from the vertical penetration effect such that the overall biases may cancel out. Indeed, the largest source of error in N_d is likely
that from r_e biases given the sensitivity of N_d to r_e in Eqn. 10. MODIS r_e has generally been shown to be biased positively
compared to aircraft observations (Painemal and Zuidema, 2011; King et al., 2012), which would lead to a negative N_d error
when taken alone. Thus, the application of the correction described in this paper in isolation has the potential to enhance any
negative bias in N_d caused by a positive r_e bias.

Painemal and Zuidema (2011) actually demonstrated that MODIS N_d agreed rather well with N_d from aircraft for the SE
Pacific region despite the fairly large r_e bias; this was thought to be due to the fortuitous cancellation of (for N_d) the r_e bias
10 with biases in the k parameter and f_{ad} . However, the agreement between aircraft and MODIS N_d seen in Painemal and Zuidema
(2011) would deteriorate if a correction for the N_d bias due to the penetration depth effect discussed here was also applied.
Table 2 indicates that the result would be a MODIS N_d underestimate of around 35 % (average for SE Pacific, region#1) for
the 2.1 μm retrieval, assuming perfect initial agreement. This indicates that another N_d bias may have been operating in order
to give the good observed agreement.

15 6 Conclusions

We have described and quantified a positive bias in satellite retrievals of cloud droplet concentration (N_d) that make use of the
adiabatic cloud assumption to estimate N_d from satellite observed cloud optical depth (τ), effective radius (r_e) and cloud top
temperature. We term the N_d bias the “vertical penetration bias”. The bias is specific to the methodology of the N_d retrieval,
as opposed to being a bias in the underlying observations. It arises due to the well-documented vertical penetration of photons
20 with wavelengths in the shortwave-infrared range into the upper regions of clouds, so that r_e retrievals are representative of
values some distance below cloud top (Platnick, 2000; Bennartz and Rausch, 2017) rather than being those at cloud top as
assumed by the N_d retrieval. Here we quantified the optical depth as measured from cloud top downwards, $d\tau$, at which the
retrieved r_e equaled the actual r_e for adiabatic clouds covering a large range of total cloud optical depths and N_d values. We
showed that knowledge of $d\tau$ allows a corrected N_d to be calculated by subtracting $d\tau$ from the observed τ and using that
25 in the N_d retrieval instead of τ . We characterised $d\tau$ as functions of τ for the 2.1 and 3.7 μm r_e retrievals ($r_{e2.1}$ and $r_{e1.6}$,
respectively) and found that a 1-D relationship approximates the modelled data well. $d\tau$ increases with τ and is larger for $r_{e2.1}$
than for $r_{e3.7}$ and so the vertical penetration N_d bias affects retrievals based on $r_{e2.1}$ more than those using $r_{e3.7}$.



We quantified the vertical penetration N_d bias for a one-year N_d data set. The new N_d formulation presented here suggests that N_d errors will increase as the τ value of the cloud scene gets lower. For many regions that are considered trustworthy for 30 N_d retrievals (typically stratocumulus regions), there are high frequencies of low τ values and so the N_d biases are significant. For example, for the SE Pacific and SE Atlantic regions clouds with $\tau \leq 10$ (for which N_d errors are expected to be $\geq 33\%$ for $r_{e2.1}$ and $\geq 15\%$ for $r_{e3.7}$) occur, respectively, 56 and 72% of the time on average. The mean $r_{e2.1}$ vertical penetration N_d biases for these regions were 35 and 38%, respectively. Out of the stratocumulus regions examined, these two were the worst affected. For $r_{e3.7}$ the N_d biases were much smaller; for example, mean biases for the SE Pacific and SE Atlantic regions were 17 and 20%, respectively. N_d biases were predicted to be worse for the tropical and sub-tropical regions than for higher latitudes. The time-variability of the biases were also examined and were shown to be significant (regional mean standard deviations of 20–40% and 40–60% for $r_{e2.1}$ and $r_{e3.7}$, respectively). This indicates that long term averages of the vertical penetration N_d bias 5 corrections are not useful for correcting N_d data over short timescales (e.g. daily N_d data). We also examined the seasonality of the N_d biases and showed that, for the stratocumulus regions, generally the DJF season was worst affected, followed by SON.

We caution that the correction for the vertical penetration N_d bias presented here should only be considered in combination with corrections for other biases that affect N_d since otherwise N_d biases could be made worse, for example in situations where the fortuitous cancellation of opposing errors leads to initially small N_d errors. The latter was suspected to have occurred for 10 the comparison between MODIS N_d retrievals and in-situ aircraft observations as presented in Painemal and Zuidema (2011). We showed that the SE Pacific, which is the region examined in that study, had a mean vertical penetration depth error of 35% suggesting that another unidentified N_d bias may have been operating in order to give good agreement.

Previous studies have shown that $r_{e3.7}$ is less prone to biases due to sub-pixel averaging (Zhang and Plantnick, 2011; Zhang et al., 2012, 2016). Thus, combined with the work presented here, this supports the conclusion that $r_{e3.7}$ likely represents a 15 better choice for use in N_d retrievals.

For future work, it is recommended that additional characterization of $d\tau$ is performed for a range of viewing geometries in order to ensure that the results presented here are robust for all cloud retrievals. Further investigation into how the presence of precipitation affects our assumptions and results is also warranted.

7 Data availability

The data set is built from publically available MODIS Level-2 data (Collection 5).

Author contributions. D. P. Grosvenor developed the concepts and ideas for the direction of the paper, performed the error calculations using 5 the MODIS data, produced the figures and wrote the manuscript. O. Sourdeval performed the retrievals upon the idealised adiabatic clouds. All authours provided additional input and comments on the paper during the paper writing process.

Competing interests. The authors declare that they have no conflict of interest.



Acknowledgements. DPG was funded by both the University of Leeds under Paul Field and from the NERC funded ACSIS programme via NCAS. OS was funded by the Federal Ministry for Education and Research in Germany (BMBF) in the High Definition Clouds and Precipitation for Climate Prediction (HD(CP)²) project (FKZ 01LK1503A and 01LK1505E). RW's contribution was supported on NASA award number NNX16AP31G. The MODIS data were obtained from NASA's Level 1 and Atmosphere Archive and Distribution System(LAADS <http://ladsweb.nascom.nasa.gov/>). NOAA_OI_SST_V2 data (SST data) was provided by the NOAA/OAR/ESRL PSD, Boulder, Colorado, USA, from their website at <http://www.esrl.noaa.gov/psd/>.



References

15 Ackerman, A. S., Kirkpatrick, M. P., Stevens, D. E., and Toon, O. B.: The impact of humidity above stratiform clouds on indirect aerosol climate forcing, *Nature*, 432, 1014–1017, doi:10.1038/nature03174, <http://dx.doi.org/10.1038/nature03174>, 2004.

Adebisi, A., Zuidema, P., and Abel, S.: The convolution of dynamics and moisture with the presence of shortwave absorbing aerosols over the southeast Atlantic, *J. Clim.*, 28, 1997–2024, doi:10.1175/JCLI-D-14-00352.1, 2015.

Ahmad, I., Mielonen, T., Grosvenor, D. P., Portin, H. J., Arola, A., Mikkonen, S., Kühn, T., Leskinen, A., Joutsensaari, J., Komppula, M.,
20 Lehtinen, K. E. J., Laaksonen, A., and Romakkaniemi, S.: Long-term measurements of cloud droplet concentrations and aerosol–cloud interactions in continental boundary layer clouds, *Tellus B*, 65, doi:10.3402/tellusb.v65i0.20138, <http://dx.doi.org/10.3402/tellusb.v65i0.20138>, 2013.

Albrecht, B. A.: Aerosols, Cloud Microphysics, and Fractional Cloudiness, *Science*, 245, 1227–1230, <http://www.jstor.org/stable/1704234>, 1989.

25 Bennartz, R.: Global assessment of marine boundary layer cloud droplet number concentration from satellite, *JOURNAL OF GEOPHYSICAL RESEARCH-ATMOSPHERES*, 112, doi:10.1029/2006JD007547, 2007.

Bennartz, R.: Global assessment of marine boundary layer cloud droplet number concentration from satellite, *J. Geophys. Res.*, 112, D02 201, doi:10.1029/2006JD007547, 2007.

Bennartz, R. and Harshvardhan: Correction to “Global assessment of marine boundary layer cloud droplet number concentration from 30 satellite”, *J. Geophys. Res.*, 112, D02 201, doi:10.1029/2007JD008841, 2007.

Bennartz, R. and Rausch, J.: Global and regional estimates of warm cloud droplet number concentration based on 13 years of AQUA-MODIS observations, *Atmos. Chem. Phys. Discuss.*, in review, doi:10.5194/acp-2016-1130, 2017.

Berner, A. H., Bretherton, C. S., Wood, R., and Muhlbauer, A.: Marine boundary layer cloud regimes and POC formation in a CRM coupled to a bulk aerosol scheme, *Atmospheric Chemistry and Physics*, 13, 12 549–12 572, doi:10.5194/acp-13-12549-2013, <http://dx.doi.org/10.5194/acp-13-12549-2013>, 2013.

35 Boers, R., Acarreta, J. R., and Gras, J. L.: Satellite monitoring of the first indirect aerosol effect: Retrieval of the droplet concentration of water clouds, *J. Geophys. Res.*, 111, D22 208, doi:10.1029/2005JD006838, 2006.

Brenguier, J., Burnet, F., and Geoffroy, O.: Cloud optical thickness and liquid water path—does the k coefficient vary with droplet concentration?, *Atmos. Chem. Phys.*, 11, 9771–9786, doi:10.5194/acp-11-9771-2011, 2011.

Brenguier, J.-L., Pawlowska, H., Schüller, L., Preusker, R., Fischer, J., and Fouquart, Y.: Radiative properties of boundary layer clouds: Droplet effective radius versus number concentration, *J. Atmos. Sci.*, 57, 803–821, doi:10.1175/1520-5469(2000)057<0803:RPOBLC>2.0.CO;2, 2000.

Bretherton, C. S., Blossey, P. N., and Uchida, J.: Cloud droplet sedimentation, entrainment efficiency, and subtropical stratocumulus albedo, *Geophysical Research Letters*, 34, n/a–n/a, doi:10.1029/2006GL027648, <http://dx.doi.org/10.1029/2006GL027648>, 2007.

Cavalieri, D. J., Parkinson, C. L., Gloersen, P., and Zwally, H. J.: Sea Ice Concentrations from Nimbus-7 SMMR and DMSP SSM/I-SSMIS Passive Microwave Data, Version 1. Boulder, Colorado USA. NASA National Snow and Ice Data Center Distributed Active Archive Center. Accessed 22nd December, 2016., doi:10.5067/8gq8lzql0vl, 1996.

10 Chang, F.-L. and Li, Z.: Estimating the vertical variation of cloud droplet effective radius using multispectral near-infrared satellite measurements, *Journal of Geophysical Research: Atmospheres*, 107, AAC 7–1–AAC 7–12, doi:10.1029/2001JD000766, <http://dx.doi.org/10.1029/2001JD000766>, 2002.



Davis, S. M., Avallone, L. M., Kahn, B. H., Meyer, K. G., and Baumgardner, D.: Comparison of airborne in situ measurements and Moderate Resolution Imaging Spectroradiometer (MODIS) retrievals of cirrus cloud optical and microphysical properties during the Midlatitude Cirrus Experiment (MidCiX), *J. Geophys. Res. Atmos.*, 114, D02 203, doi:10.1029/2008JD010284, 2009.

Di Girolamo, L., Liang, L., and Platnick, S.: A global view of one-dimensional solar radiative transfer through oceanic water clouds, *GEOPHYSICAL RESEARCH LETTERS*, 37, doi:10.1029/2010GL044094, 2010.

Feingold, G., Koren, I., Yamaguchi, T., and Kazil, J.: On the reversibility of transitions between closed and open cellular convection, *Atmospheric Chemistry and Physics*, 15, 7351–7367, doi:10.5194/acp-15-7351-2015, <http://dx.doi.org/10.5194/acp-15-7351-2015>, 2015.

Grosvenor, D. P. and Wood, R.: The effect of solar zenith angle on MODIS cloud optical and microphysical retrievals within marine liquid water clouds, *Atmospheric Chemistry and Physics*, 14, 7291–7321, doi:10.5194/acp-14-7291-2014, <http://www.atmos-chem-phys.net/14/7291/2014/>, 2014.

Han, Q., Rossow, W., Chou, J., and Welch, R.: Global variations of column droplet concentration in low-level clouds, *Geophys. Res. Lett.*, 25, 1419–1422, doi:10.1029/98GL01095, 1998.

Hartmann, D. L., Ockert-Bell, M. E., and Michelsen, M. L.: The Effect of Cloud Type on Earth's Energy Balance: Global Analysis, *Journal of Climate*, 5, 1281–1304, doi:10.1175/1520-0442(1992)005<1281:teocto>2.0.co;2, [http://dx.doi.org/10.1175/1520-0442\(1992\)005<1281:teocto>2.0.co;2](http://dx.doi.org/10.1175/1520-0442(1992)005<1281:teocto>2.0.co;2), 1992.

Haywood, J. M., Osborne, S. R., and Abel, S. J.: The effect of overlying absorbing aerosol layers on remote sensing retrievals of cloud effective radius and cloud optical depth, *Q. J. R. Meteorol. Soc.*, 130, 779–800, doi:10.1256/qj.03.100, 2004.

Hill, A. A., Feingold, G., and Jiang, H.: The Influence of Entrainment and Mixing Assumption on Aerosol–Cloud Interactions in Marine Stratocumulus, *Journal of the Atmospheric Sciences*, 66, 1450–1464, doi:10.1175/2008jas2909.1, <http://dx.doi.org/10.1175/2008JAS2909.1>, 2009.

Horváth, Á.: Anisotropy of water cloud reflectance: A comparison of measurements and 1D theory, *Geophysical Research Letters*, 31, doi:10.1029/2003gl018386, <https://doi.org/10.1029/2003gl018386>, 2004.

Janssen, R. H. H., Ganzeveld, L. N., Kabat, P., Kulmala, M., Nieminen, T., and Roebeling, R. A.: Estimating seasonal variations in cloud droplet number concentration over the boreal forest from satellite observations, *Atmos. Chem. Phys.*, 11, 7701–7713, doi:10.5194/acp-11-7701-2011, 2011.

Kato, S. and Marshak, A.: Solar zenith and viewing geometry-dependent errors in satellite retrieved cloud optical thickness: Marine stratocumulus case, *J. Geophys. Res.*, 114, D01 202, doi:10.1029/2008JD010579, 2009.

King, M. D., Tsay, S.-C., Platnick, S. E., Wang, M., and Liou, K. N.: Cloud retrieval algorithms for MODIS. Optical thickness, effective particle radius, and thermodynamic phase., NASA, MODIS Algorithm Theoretical Basis document No. ATBD-MOD-05, 1997.

King, N. J., Bower, K. N., Crosier, J., and Crawford, I.: Evaluating MODIS cloud retrievals with in situ observations from VOCALS-REx, *Atmospheric Chemistry and Physics Discussions*, 12, 23 679–23 729, doi:10.5194/acpd-12-23679-2012, <http://www.atmos-chem-phys-discuss.net/12/23679/2012/>, 2012.

Latham, J., Rasch, P., Chen, C.-C., Kettles, L., Gadian, A., Gettelman, A., Morrison, H., Bower, K., and Choularton, T.: Global temperature stabilization via controlled albedo enhancement of low-level maritime clouds, *Philosophical Transactions of the Royal Society A: Mathematical, Physical and Engineering Sciences*, 366, 3969–3987, doi:10.1098/rsta.2008.0137, <http://dx.doi.org/10.1098/rsta.2008.0137>, 2008.



Liang, L. and Girolamo, L. D.: A global analysis on the view-angle dependence of plane-parallel oceanic liquid water cloud optical thickness
15 using data synergy from MISR and MODIS, *Journal of Geophysical Research: Atmospheres*, pp. n/a–n/a, doi:10.1029/2012JD018201,
<http://dx.doi.org/10.1029/2012JD018201>, 2013.

Liang, L., Di Girolamo, L., and Platnick, S.: View-angle consistency in reflectance, optical thickness and spherical albedo of marine water-
clouds over the northeastern Pacific through MISR-MODIS fusion, *Geophys. Res. Lett.*, 36, doi:10.1029/2008GL037124, 2009.

Liang, L., Girolamo, L. D., and Sun, W.: Bias in MODIS cloud drop effective radius for oceanic water clouds as deduced from optical thick-
20 ness variability across scattering angles, *Journal of Geophysical Research: Atmospheres*, 120, 7661–7681, doi:10.1002/2015jd023256,
<https://doi.org/10.1002/2015jd023256>, 2015.

Maddux, B. C., Ackerman, S. A., and Platnick, S.: Viewing Geometry Dependencies in MODIS Cloud Products, *JOURNAL OF ATMO-
SPHERIC AND OCEANIC TECHNOLOGY*, 27, 1519–1528, 2010.

Marshak, A., Platnick, S., Varnai, T., Wen, G., and Cahalan, R.: Impact of three-dimensional radiative effects on satellite retrievals of cloud
25 droplet sizes, *JOURNAL OF GEOPHYSICAL RESEARCH-ATMOSPHERES*, 111, doi:10.1029/2005JD006686, 2006.

Martin, G., JOHNSON, D., and SPICE, A.: THE MEASUREMENT AND PARAMETERIZATION OF EFFECTIVE RADIUS
OF DROPLETS IN WARM STRATOCUMULUS CLOUDS, *JOURNAL OF THE ATMOSPHERIC SCIENCES*, 51, 1823–1842,
doi:10.1175/1520-0469(1994)051<1823:TMAPOE>2.0.CO;2, 1994.

Merk, D., Deneke, H., Pospichal, B., and Seifert, P.: Investigation of the adiabatic assumption for estimating cloud micro- and macrophysical
30 properties from satellite and ground observations, *Atmos. Chem. Phys.*, 16, 933–952, doi:10.5194/acp-16-933-2016, 2016.

Meyer, K., Platnick, S., Oreopoulos, L., and Lee, D.: Estimating the direct radiative effect of absorbing aerosols overlying marine boundary
layer clouds in the southeast Atlantic using MODIS and CALIOP, *J. Geophys. Res.*, 118, 4801–4815, doi:10.1002/jgrd.50449, 2013.

Nakajima, T., Higurashi, A., Kawamoto, K., and Penner, J. E.: A possible correlation between satellite-derived cloud and aerosol microphys-
ical parameters, *Geophys. Res. Lett.*, 28, 1171–1174, doi:10.1029/2000GL012186, 2001.

Nakajima, T. Y., Suzuki, K., and Stephens, G. L.: Droplet Growth in Warm Water Clouds Observed by the A-Train. Part I: Sen-
35 sitivity Analysis of the MODIS-Derived Cloud Droplet Sizes, *JOURNAL OF THE ATMOSPHERIC SCIENCES*, 67, 1884–1896,
doi:10.1175/2009JAS3280.1, 2010a.

Nakajima, T. Y., Suzuki, K., and Stephens, G. L.: Droplet Growth in Warm Water Clouds Observed by the A-Train. Part II: A Multisensor
View, *JOURNAL OF THE ATMOSPHERIC SCIENCES*, 67, 1897–1907, doi:10.1175/2010JAS3276.1, 2010b.

Oreopoulos, L.: The impact of subsampling on MODIS Level-3 statistics of cloud optical thickness and effective radius, *IEEE TRANSAC-
TIONS ON GEOSCIENCE AND REMOTE SENSING*, 43, 366–373, doi:10.1109/TGRS.2004.841247, 2005.

Painemal, D. and Zuidema, P.: Assessment of MODIS cloud effective radius and optical thickness retrievals over the Southeast Pacific with
VOCALS-REx in situ measurements, *JOURNAL OF GEOPHYSICAL RESEARCH-ATMOSPHERES*, 116, doi:10.1029/2011JD016155,
2011.

Pawlowska, H., Grabowski, W. W., and Brenguier, J.-L.: Observations of the width of cloud droplet spectra in stratocumulus, *Geophysical
Research Letters*, 33, doi:10.1029/2006gl026841, <https://doi.org/10.1029%2F2006gl026841>, 2006.

Platnick, S.: Vertical photon transport in cloud remote sensing problems, *JOURNAL OF GEOPHYSICAL RESEARCH-ATMOSPHERES*,
105, 22 919–22 935, doi:10.1029/2000JD900333, 2000.

Quaas, J., Boucher, O., and Lohmann, U.: Constraining the total aerosol indirect effect in the LMDZ and ECHAM4 GCMs using MODIS
satellite data, *Atmos. Chem. Phys.*, 6, 947–955, doi:10.5194/acp-6-947-2006, 2006.



15 Salomonson, V. V., Barnes, W. L., Maymon, P. W., Montgomery, H. E., and Ostrow, H.: MODIS: advanced facility instrument for studies of the Earth as a system, *IEEE Transact. Geosci. Remote Sens.*, 27, 145–153, doi:10.1109/36.20292, 1998.

Sourdeval, O., Labonne, L. C., Brogniez, G., Jourdan, O., Pelon, J., and Garnier, A.: A variational approach for retrieving ice cloud properties from infrared measurements: application in the context of two IIR validation campaigns, *Atmos. Chem. Phys.*, 13, 8229–8244, doi:10.5194/acp-13-8229-2013, 2013.

20 Sourdeval, O., C. Labonne, L., Baran, A. J., Mülmenstädt, J., and Brogniez, G.: A methodology for simultaneous retrieval of ice and liquid water cloud properties. Part 2: Near-global retrievals and evaluation against A-Train products, *Quarterly Journal of the Royal Meteorological Society*, 142, 3063–3081, doi:10.1002/qj.2889, 2016.

Stamnes, K., Tsay, S. C., Wiscombe, W., and Jayaweera, K.: Numerically stable algorithm for discrete-ordinate-method radiative transfer in multiple scattering and emitting layered media, *Appl. Opt.*, 27, 2502–2509, 1988.

25 Stevens, B., Cotton, W. R., Feingold, G., and Moeng, C.-H.: Large-Eddy Simulations of Strongly Precipitating, Shallow, Stratocumulus-Topped Boundary Layers, *J. Atmos. Sci.*, 55, 3616–3638, doi:10.1175/1520-0469(1998)055<3616:lesosp>2.0.co;2, [http://dx.doi.org/10.1175/1520-0469\(1998\)055<3616:LESOSP>2.0.CO;2](http://dx.doi.org/10.1175/1520-0469(1998)055<3616:LESOSP>2.0.CO;2), 1998.

Suzuki, K., Nakajima, T. Y., and Stephens, G. L.: Particle Growth and Drop Collection Efficiency of Warm Clouds as Inferred from Joint-CloudSat and MODIS Observations, *Journal of the Atmospheric Sciences*, 67, 3019–3032, doi:10.1175/2010jas3463.1, <https://doi.org/10.1175/2010jas3463.1>, 2010.

30 Szczodrak, M., Austin, P., and Krummel, P.: Variability of optical depth and effective radius in marine stratocumulus clouds, *J. Atmos. Sci.*, 58, 2912–2926, doi:10.1175/1520-0469(2001)058<2912:VOODAE>2.0.CO;2, 2001.

Twomey, S.: Pollution and the planetary albedo, *Atmos. Environ.*, 8, 1251–1258, doi:10.1016/0004-6981(74)90004-3, 1974.

van de Hulst, H.: Light Scattering by small particles, Dover Publications, New York, 1957.

Várnai, T. and Davies, R.: Effects of Cloud Heterogeneities on Shortwave Radiation: Comparison of Cloud-Top Variability and Internal 35 Heterogeneity, *J. Atmos. Sci.*, 56, 4206–4224, doi:10.1175/1520-0469(1999)056<4206:EOCHOS>2.0.CO;2, 1999.

Várnai, T. and Marshak, A.: View angle dependence of cloud optical thicknesses retrieved by Moderate Resolution Imaging Spectroradiometer (MODIS), *JOURNAL OF GEOPHYSICAL RESEARCH-ATMOSPHERES*, 112, doi:10.1029/2005JD006912, 2007.

Zhang, Z.: On the sensitivity of cloud effective radius retrieval based on spectral method to bi-modal droplet size distribution: A semi-analytical model, *Journal of Quantitative Spectroscopy and Radiative Transfer*, 129, 79–88, doi:10.1016/j.jqsrt.2013.05.033, <http://dx.doi.org/10.1016/j.jqsrt.2013.05.033>, 2013.

480 Zhang, Z. and Plantnick, S.: An assessment of differences between cloud effective particle radius retrievals for marine water clouds from three MODIS spectral bands, *JOURNAL OF GEOPHYSICAL RESEARCH-ATMOSPHERES*, 116, 2011.

Zhang, Z., Werner, F., Cho, H. M., Wind, G., Platnick, S., Ackerman, A. S., Di Girolamo, L., Marshak, A., and Meyer, K.: A framework based on 2-D Taylor expansion for quantifying the impacts of subpixel reflectance variance and covariance on cloud optical thickness and effective radius retrievals based on the bispectral method, *J. Geophys. Res. Atmos.*, 121, 7007–7025, doi:10.1002/2016JD024837, 2016.

Zhang, Z., Ackerman, A. S., Feingold, G., Platnick, S., Pincus, R., and Xue, H.: Effects of cloud horizontal inhomogeneity and drizzle on remote sensing of cloud droplet effective radius: Case studies based on large-eddy simulations, *JOURNAL OF GEOPHYSICAL RESEARCH-ATMOSPHERES*, 117, doi:10.1029/2012JD017655, 2012.

Zuidema, P., Painemal, D., de Szeke, S., and Fairall, C.: Stratocumulus Cloud-Top Height Estimates and Their Climatic Implications, 490 Journal of Climate, 22, 4652–4666, doi:10.1175/2009JCLI2708.1, <http://dx.doi.org/10.1175/2009JCLI2708.1>, 2009.